

# Turbine Blade of Gas Turbine Engine Additional Unloading by Changing the Layout of the Gravity Centre of the Shroud Shelf

Ēriks Ozoliņš<sup>1</sup>, Ilmārs Ozoliņš<sup>2</sup>, Līga Ramāna<sup>3</sup>

<sup>1,2</sup>Institute of Aeronautics, Faculty of Transport and Mechanical Engineering, Transport and Aeronautics, Riga Technical University, Riga, Latvia

<sup>3</sup>Institute of Applied Mathematics, Faculty of Computer Science and Information Technology, Riga Technical University, Riga, Latvia

**Abstract** – The article describes the impact of the gas turbine engine low-pressure turbine blade shroud shelf on the blade profile stress position. Attention is focused directly on the impact of the location of the gravity centre of the shroud shelf on blade stress distribution at the three most critical points of the profile. The paper describes the details of the calculation and the required expressions provided, as well as the results of the calculation example with clear graphical dependencies.

**Keywords** – Turbine blade, shroud shelf, blade load removing.

## I. INTRODUCTION

The turbine blades are exposed to heavy working conditions. Blades of the modern gas turbine engines often contain shroud shelves (see Fig. 1a). Due to this fact aircraft manufacturing companies choose such blades in low-pressure turbines. Shroud shelves increase the rigidity of blades and ensure gas flow sealing. But an increased load of the blade resulting from additional mass within the maximum radius of the rotor may be mentioned as a deficiency [1]–[3]. The additional centrifugal forces increase the stress level in the aerodynamically profiled part of the blade including its profile root part.

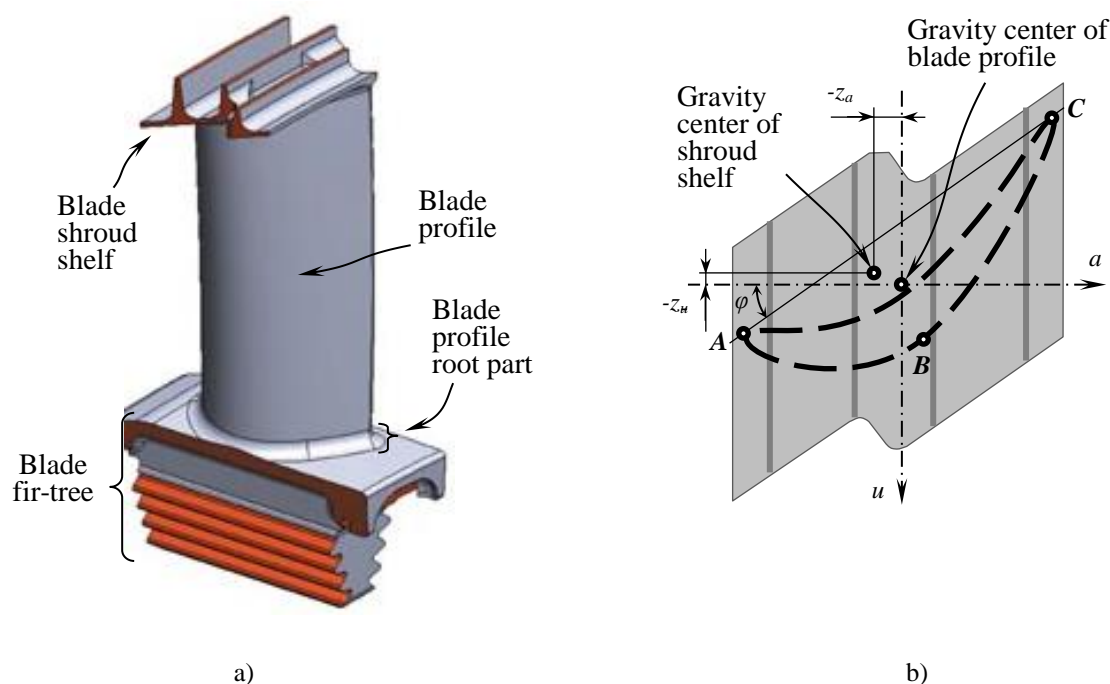


Fig. 1. Turbine blade with shroud shelf (a) and overview of the blade from above (b), where  $a$  – rotor axis;  $u$  – circumferential axis.

This paper discusses the possibility for load reduction of aerodynamically profiled part of a gas turbine engine turbine non-refrigerated blade by changing the location of the gravity centre of the shroud shelf (see Fig. 1b). The optimal unload can be observed if a combination of different load reduction options is applied, which requires rather extensive calculation studies. The study was limited to the replacement of the gravity centre of the shroud shelf in the direction of the rotor axis and the circumferential. In that way contributing to the aerodynamically profiled part of the blade in the medium-radius area in addition to the residual bending forces (followed by bending stress) which remain after removing the base load with skewed method. Even such a small load reduction can extend the lifetime of the blade and increase the overall safety of the structure. The study carried out on classical expressions of static strength, so appropriate assumptions have been made. The paper shows main equations for static forces, moments and stresses generated with them, provides the results of the calculation sample and possible directions for further studies. The study can be useful for those interested in calculating algorithms that want to gain an in-depth understanding of the specifics, nuances and challenges of calculating a complex detail.

## II. BLADE WITH SHROUD SHELF PROFILE PART UNLOADING WITH SKEWED METHOD

The initial data corresponds to a classic calculation case, which were: rotor rotation speed, blade material density, rotor diameter, geometrical dimensions of the blade, and degree gas dynamic values of the rotor stage [1].

The following assumptions had been taken for the calculation of the blade profile strength [2], [3]:

- the blade attached in the form of a console;
- the blade is rigid;
- thermal stresses are not taken into account;
- stresses do not exceed the elastic limit of blade material;
- the blade attachment to the disc rim is rigid;
- torsion tangential stresses are not taken into account (blade profile stiffness centres are assumed to coincide with pressure centres).

As a result, the bending stresses from the gas forces and the tensile and bending stresses from the centrifugal forces was considered in the blade. The assumptions given allow to focus more attention on the subject and avoid the labour-intensive calculations.

Before applying to the blade in addition to the load reduction calculations related to the layout of the gravity centre of the shroud shelf, an initial calculation option was selected, which was a model for further calculations. A description of the course of the basic and load reduction calculation of the blade with the shroud shelf was not the purpose of the given study, which can be found in many literature sources [4]–[16].

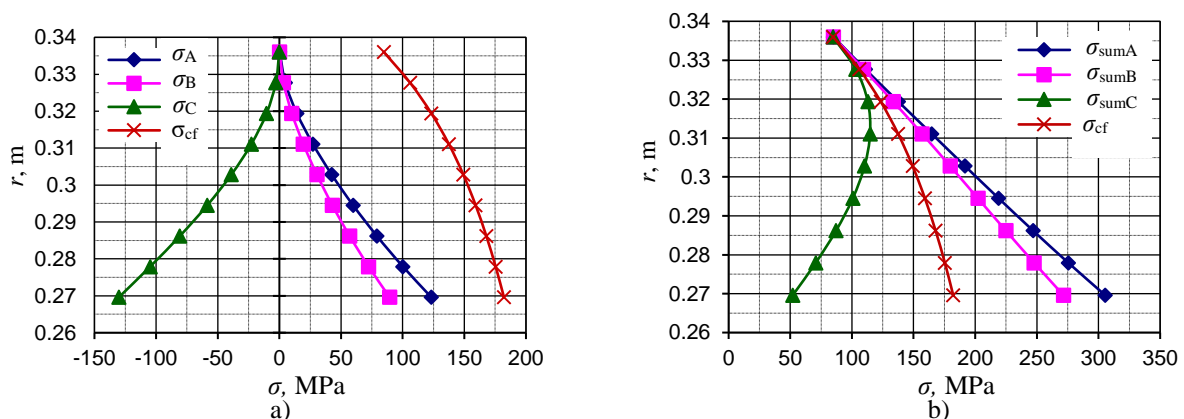


Fig. 2 The distribution of the bending (a) and the total (b) stresses along the blade length before stress reduction of the root part of the blade considering the impact of the shroud shelf;  $\sigma_A$ ,  $\sigma_B$  and  $\sigma_C$  – bending stresses in profile points A, B and C accordingly;  $\sigma_{sumA}$ ,  $\sigma_{sumB}$  and  $\sigma_{sumC}$  – bending and circumferential total stresses in profile points A, B and C accordingly;  $\sigma_{cf}$  – circumferential force created stresses.

The further calculations related to the shroud shelf on the results obtained by the methodology are described at work [1]. Fig. 2 shows the breakdown of the stresses of chosen blade along the length of the blade before it was unloaded from bending stresses.

The load reduction was realised only by tilting the blade in the required direction at an angle size  $\alpha$  (see Fig. 4) without bending the profiled part (Table I).

In contrast to the bench mode, in the cruising mode, the centrifugal and gas forces change as the engine operating mode (rotor rotation speed) and airflow parameters at the engine entrance change. Therefore, load removing coefficient  $\zeta$  should be introduced, which provides these changes ensuring a maximum unload directly in the cruising mode. For the simplification of the given calculation the coefficient  $\zeta = 1$  is accepted (assume that the calculation was carried out directly for the cruising mode).

TABLE I  
BLADE SKEW ANGLES

Rotor axial direction			Rotor circumferential direction		
$\alpha, ^\circ$	$\cos\alpha$	$\sin\alpha$	$\alpha, ^\circ$	$\cos\alpha$	$\sin\alpha$
88.56804	0.02499	0.99969	85.94508	0.07071	0.99749

After the blade load reduction calculation [1] the stresses dependencies shown in Fig. 3 were derived.

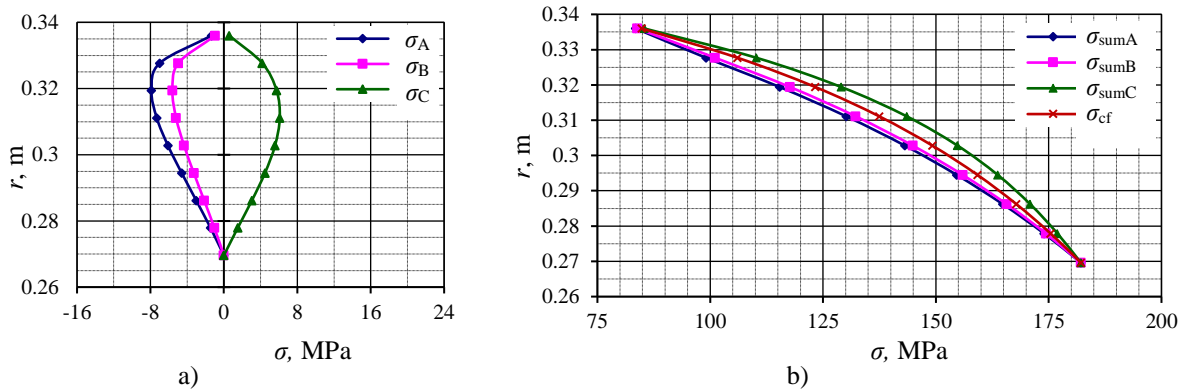


Fig. 3. The distribution of the bending (a) and the total (b) stresses along the blade length after stress reduction of the root part of the blade considering the impact of the shroud shelf;  $\sigma_A$ ,  $\sigma_B$  and  $\sigma_C$  – bending stresses in profile points A, B and C accordingly;  $\sigma_{sumA}$ ,  $\sigma_{sumB}$  and  $\sigma_{sumC}$  – bending and circumferential total stresses in profile points A, B and C accordingly;  $\sigma_{cf}$  – circumferential force created stresses.

There is a stratification of the stress distribution curves in the profile points A, B and C. It is mostly caused by the shroud shelf. The centrifugal force created by the shroud shelf was concentrated at the end of the blade. It changes the force, thus also the moment, the balance along the length of the blade [1]. The shroud shelf also changes the bending stress marks. In point C, the tensile stresses and, in points A and B, the compressive stresses are generated. The residual bending (following also the sum) stresses are observed at the profile points C in the middle of the blade (particularly radius  $r = 0.3 \dots 0.325$ ) after the blade load reduction can be observed (see Fig. 3a). These residual stresses that attempted to be reduce by operating with the change in the mass centre of the shroud shelf, which was examined in Chapter III. It can be concluded that there is such a mass of the shroud shelf at which the degree of stratification of the stress curves tends to zero. But due to the limit of the study it was decided to operate only with the coordinates of the centre of gravity of the shroud shelf, assuming that mass cannot be reduced.

### III. PROFILE PART LOAD REDUCTION WITH CHANGE OF THE SHROUD SHELF MASS CENTRE

The shroud shelf was not calculated. In addition to the input data previously accepted (Chapter II), the coordinates of the shroud shelf gravity centre ( $z_a$  and  $z_u$ ) was entered. The calculation pattern in the direction of the rotor axis is shown in Fig. 4. For a more comfortable explanation of the calculation phase, the blade was divided into 4 parts (5 slices) (see Fig. 4). [1]. But the numerical results in tables and graphics was displayed from 9 section calculation version. The purpose of the task was to determine the angle of the blade tilt  $\alpha$ , which results in the most congested section of the blade

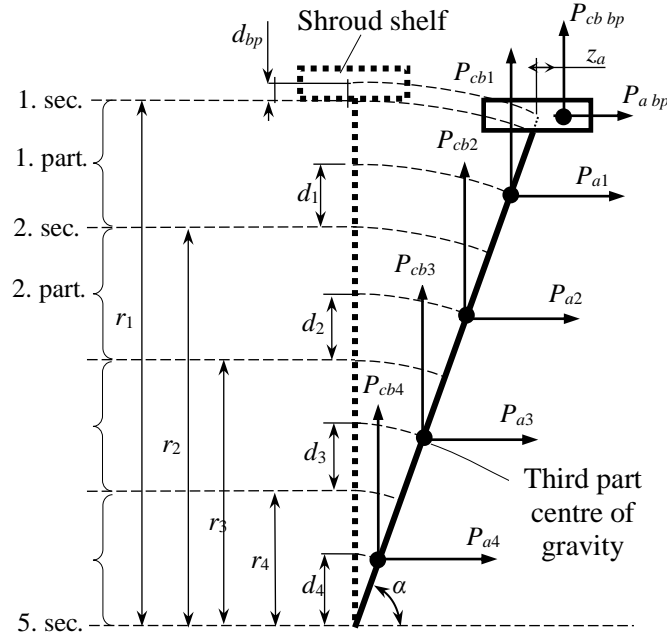


Fig. 4. Blade with shroud shelf scheme in straight position and position when the blade is tilted in the direction of the rotor axis.

(in this example, section 5) being completely unloaded, and to select shoulder  $z_a$  and  $z_u$  that relieves the midsection of the blade from residual bending stresses. It is to reduce the tensile stresses at profile points C (see Fig. 3).

For the determination of the skewing angle  $\alpha$ , for example in the direction of the rotor axis, a moment equation was used [1]:

$$\sum_{i=1}^5 M_{cb r} = \sum_{i=1}^5 M_{a r}, \quad (1)$$

where

$M_{cb r}$  – centrifugal force created bending moment in section  $r$ ;

$M_{a r}$  – the gas forces created bending moment which directed in the axis direction in section  $r$ .

When expressing moments with force and shoulder products, in addition the coordinate  $z_a$  of the shroud shelf mass centre was included (see Fig. 4). An analogous equation is for the circumferential direction (not reported).

$$\begin{aligned} & P_{a_{bp}}(r_1 + d_{bp}) \sin \alpha + P_{a_1}(r_2 + d_1) \sin \alpha + P_{a_2}(r_3 + d_2) \sin \alpha + \\ & + P_{a_3}(r_4 + d_3) \sin \alpha + P_{a_4}d_4 \sin \alpha = P_{cb_{bp}}(z_a + (r_1 + d_{bp}) \cos \alpha) + P_{cb_1}(r_2 + d_1) \cos \alpha + \\ & + P_{cb_2}(r_3 + d_2) \cos \alpha + P_{cb_3}(r_4 + d_3) \cos \alpha + P_{cb_4}d_4 \cos \alpha \end{aligned} \quad (2)$$

After putting outside of the brackets  $\sin\alpha$  and  $\cos\alpha$  and when equating to zero:

$$\begin{aligned} & \sin\alpha (P_{a\,bp}(r_1 + d_{bp}) + P_{a1}(r_2 + d_1) + P_{a2}(r_3 + d_2) + P_{a3}(r_4 + d_3) + P_{a4}d_4) - \\ & - P_{cb\,bp} \cdot z_a - \cos\alpha \left( (r_1 + d_{bp}) - P_{cb1}(r_2 + d_1) - \right. \\ & \left. - P_{cb2}(r_3 + d_2) - P_{cb3}(r_4 + d_3) - P_{cb4}d_4 \right) = 0 \end{aligned} \quad (3)$$

There are two unknown  $\alpha$  and  $z_a$  in the equation. The size  $z_a$  was initially selected freely, based solely on logic considerations, and the optimal value of that size can be found further. Angles  $\alpha$  cannot be found directly through the given equation. In this case, a sequential approximation method was applied, such as the programming language Matlab. Therefore, at the choice of  $z_a$ , the angle  $\alpha$  values were selected sequentially in the (3) and calculations made until both sides of the (3) become equal to 0. The same calculation procedure carried out in the circumferential plane of the rotor, selecting the shoulder  $z_u$  and the angles  $\alpha$ . The samples of the results shown below were calculated at the selected shoulder sizes  $z_a = 0$  and  $z_u = -0.0008$  m.

Table II shows the results of the calculation example executed in the rotor axis and in the circumferential directions as well.

TABLE II  
BLADE SKEW ANGLES

Rotor axial direction				Rotor circumferential direction			
$z_a$ , m	$\alpha$ , °	$\cos\alpha$	$\sin\alpha$	$z_u$ , m	$\alpha$ , °	$\cos\alpha$	$\sin\alpha$
0	88.56804	0.02499	0.99969	-0.0008	85.73889	0.07430	0.99723

Compared to the blade for which the shroud shelf was arranged symmetrically (see Table I), the angle  $\alpha$  of the blade with the unsymmetrically arranged shroud shelf centres of gravity in the rotor axis direction was the same because the shoulder was left unchanged at  $z_a = 0$ . While the angle of tilting  $\alpha$  was slightly reduced from  $85.9451^\circ$  to  $85.7389^\circ$ , i.e. 0.24 %, introduced by shoulder  $z_u = -0.0008$  m.

The final phase of the calculation was related to the calculation of the stress values for the blade, which was unloaded in both the base part of the blade and in the midsection. In addition, the stress values were the resultant values, including forces operating both in the rotor axis direction and in the circumferential direction. The calculation carried out for all nine sections. For this purpose, the calculation of the bending moment  $M_x$  and  $M_y$  in relation to the central inertia axis x and y, the difference of bending moments created by gas forces and centrifugal forces used:

$$M_x = (M_a - M_{cb}) \cdot \cos\varphi + (M_u - M_{cb}) \cdot \sin\varphi; \quad (4)$$

$$M_y = -(M_a - M_{cb}) \cdot \sin\varphi + (M_u - M_{cb}) \cdot \cos\varphi, \quad (5)$$

where  $\varphi$  – the angle between the blade profile horde and the rotor axis (see Fig. 1b).

The calculated moment values are shown in Table III.

TABLE III  
BENDING MOMENT VALUES

Section	Rotor axial direction		Rotor circumferential direction		$M_x, N\cdot m$	$M_y, N\cdot m$
	$M_u, N\cdot m$	$M_{cb}, N\cdot m$	$M_a, N\cdot m$	$M_{cb}, N\cdot m$		
1	0.01591	0.08582	0.03666	-2.79740	2.42714	-1.47777
2	0.48484	1.04785	1.18124	0.06297	0.74705	-1.04824
3	1.60585	2.38070	4.00457	4.02592	-0.32368	-0.66247
4	3.36329	4.13136	8.56525	9.23113	-0.87992	-0.33432
5	5.74144	6.35234	14.92668	15.83472	-1.03264	-0.07670
6	8.72451	9.10099	23.15708	24.00721	-0.90223	0.09801
7	12.29669	12.43883	33.32954	33.93155	-0.61108	0.17753
8	16.44213	16.43089	45.52202	45.80105	-0.27595	0.14929
9	21.14499	21.14499	59.81739	59.81739	2.12E-08	-1.06E-08

From the table the bending moments created by gas forces and centrifugal forces on the base section (at 9<sup>th</sup> section) coincide, the following bending moments  $M_x$  and  $M_y$  in these sections is equal to 0. The bending stresses was calculated on each section:

$$\sigma_i = \left( \frac{M_x}{I_x} \cdot Y_i + \frac{M_y}{I_y} \cdot X_i \right) \cdot 10^{-6}, \tag{6}$$

where the index  $i$  – the point of the profile, which corresponds, to points A, B and C. The inertia moments  $I_x$  and  $I_y$ , and the coordinates of profile points  $X_A, Y_A, X_B, Y_B, X_C, Y_C$ , after the unloading of the blade, although minor but change, was not considered for the simplification of the calculation.

Finally, the sum stresses calculated for each section:

$$\sigma_{sum\ i} = \sigma_i + \sigma_{cf}, \tag{7}$$

where  $\sigma_{cf}$  – tensile stresses caused by centrifugal forces.

Fig. 5 shows the bending ( $\sigma$ ) and total ( $\sigma_{sum}$ ) stress graphics resulting from the calculations along the length  $r$  of the blade. The graphics show a picture of the stress breakdown along the length of the blade. It is possible to determine the stratification degree of curves as a percentage of each section.

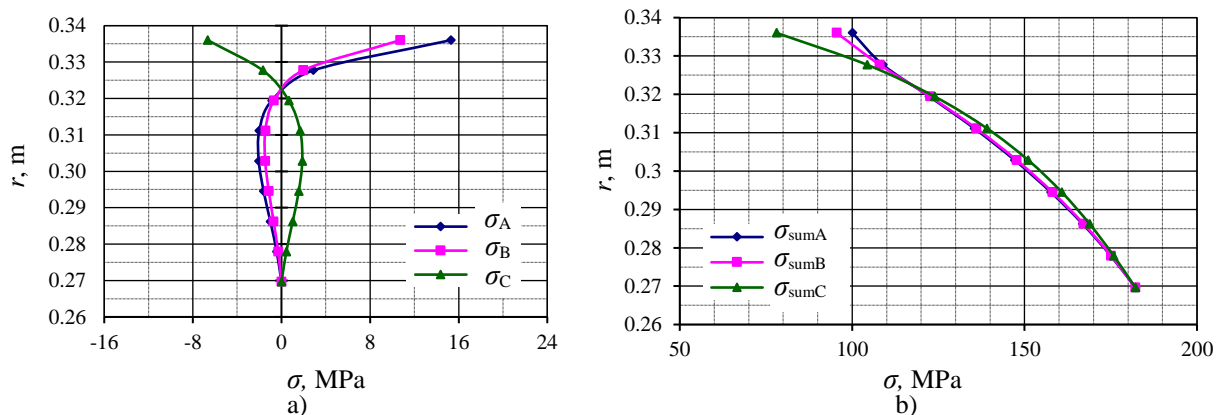


Fig. 5. The distribution of bending (a) and total (b) stresses along the length of the blade, the root part of which was reloaded, taking into account the unsymmetrical position of the gravity centre of shroud shelf;  $\sigma_A$   $\sigma_B$  and  $\sigma_C$ , – bending stresses in profile points A, B and C accordingly;  $\sigma_{sumA}$ ,  $\sigma_{sumB}$  and  $\sigma_{sumC}$  – bending and circumferential total stresses in profile points A, B and C accordingly;  $\sigma_{cf}$  – circumferential force created stresses.

Fig. 5a shows that the difference in bending stresses in the lower and medium part of the blade is insignificant. There are no bending stresses on the base part of the blade, which also met the condition

of unloaded blade. In addition, reduced stratification of curves in the blade middle part, followed in this area, compared to a symmetrically arranged shroud shelf (see Fig. 3). residual tensile stresses at profile points C were further reduced, which was also the purpose of the study.

The top of the blade showed the stratification of curves. In addition, at the upper section of the blade, the bending stresses at the profile points A and B increase similarly (Fig. 5a), while the pressure stresses at point C are increasing. As a result, the maximum tensile stress on the upper end of the blade with the non-symmetrical position of the gravity centre of the shroud shelf is 26 times higher than the blade with the symmetrical position of the gravity centre of the shroud shelf, but the average part of the blade was unloaded approximately 3.25 times, and this mean part includes a rather significant area of the blade ( $r = 0.28 \dots 0.325$ ). Even though the increase in stresses in general is more than a decrease, here, a very important role is played just where there are stresses increases and where decreases. In our case, the safety of the blade increases by applying a non-symmetrical placement of the gravity centre of the shroud shelf, because the stress level is reduced directly on the more congested part of the blade (in our case in the middle), despite significantly higher stress levels in the poorly loaded blade part (top). In other words, by operating with the coordinates of the gravity centre of the shroud shelf, it is possible to transfer part of the load from the most heavily loaded area of the blade to the less loaded area of the blade.

In addition, the calculation did not consider the rounding in the connection between the shroud shelf and the upper end of the blade section, which substantially removes the stresses, following the stress jump at the end of the blade would be significantly more moderate. In turbines with longer spades, the residual bending stress load removal effect is greater than that given in the calculation, with a length of only 0.0664 m. Of course, it is possible to choose and study the coordinates of the gravity centre ( $z_a$  and  $z_u$ ) of the shroud shelf in a wide range and combinations. Fig. 6 shows the breakdowns of bending ( $\sigma$ ) and total ( $\sigma_{\text{sum}}$ ) stresses at eight different gravity centre coordinate combinations:  $z_a = 0$  m.  $z_u = 0$ ;  $z_a = -0.0007$  m,  $z_u = 0$  m;  $z_a = -0.0014$  m,  $z_u = 0$  m;  $z_a = 0$  m.  $z_u = -0.0005$  m;  $z_a = 0$  m.  $z_u = -0.001$  m;  $z_a = -0.0005$  m,  $z_u = -0.0005$  m;  $z_a = -0.0007$  m,  $z_u = -0.0007$  m. The  $z_u$  coordinate has a greater impact on the stress distribution than the coordinate  $z_a$ , while the change in the two coordinates gives the greatest effect. Any alloy is not completely rigid following a shroud shelf with an unsymmetrically deployed gravity centre will also have an unsymmetrical elastic deformation.

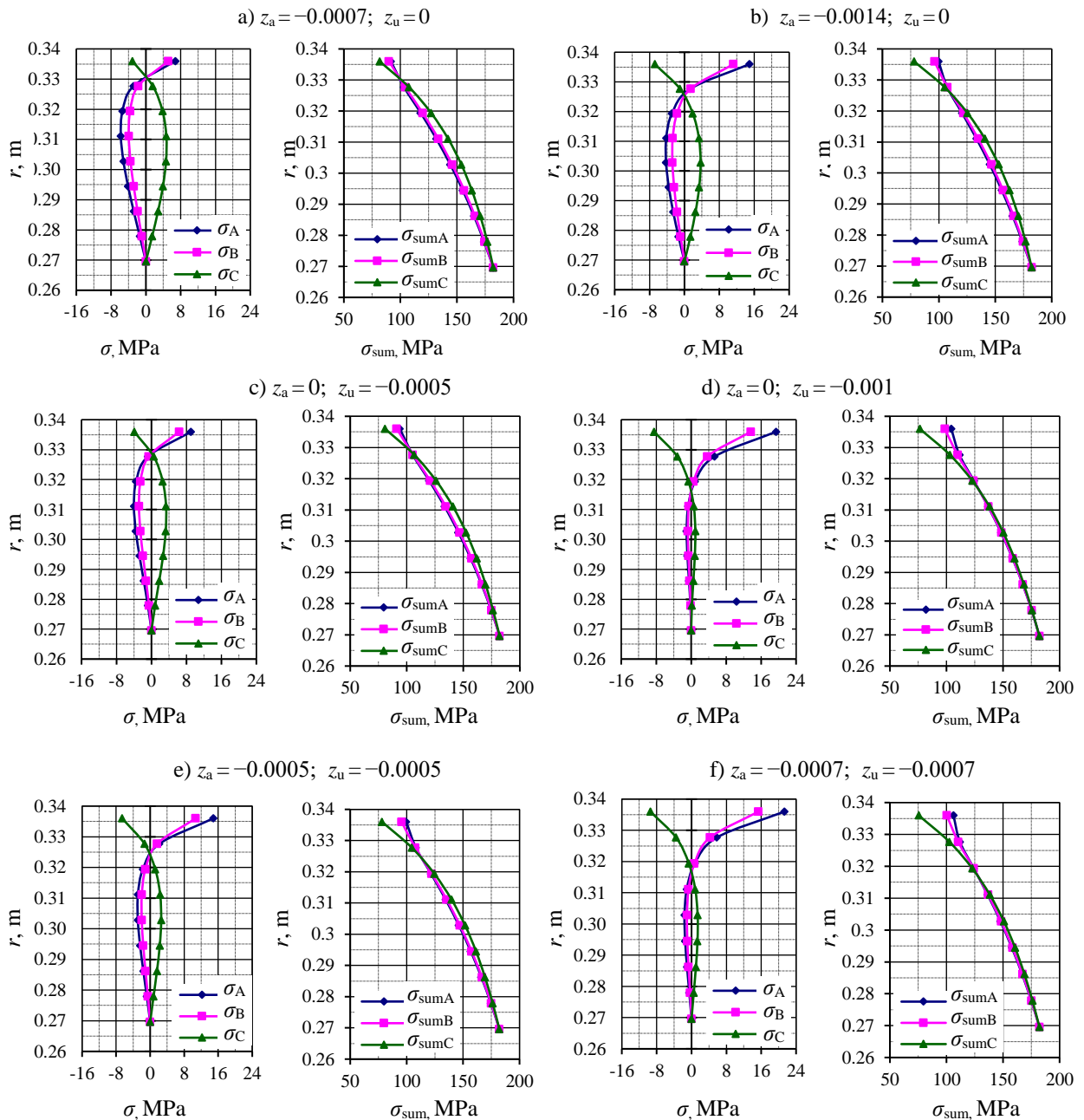


Fig. 6. Bending (a) and total (b) stresses distribution along the blade length after stress reduction considering the asymmetric centre of gravity position of the shroud shelf ( $z_a, z_u$ ), where  $\sigma_A, \sigma_B$  and  $\sigma_C$  – bending stresses in profile points A, B and C accordingly;  $\sigma_{sumA}, \sigma_{sumB}$  and  $\sigma_{sumC}$  – bending and circumferential total stresses in profile points A, B and C accordingly.

Blade shroud shelves form close contact with each other with a certain bulge size in the collision surfaces during engine operation. When the engine working conditions change, the adjacent shroud shelves with an asymmetrical gravity centre position ( $z_u$ ) will be subjected to different sizes deformations. These deformations may be minor, but in the contact surfaces of both shelves may result in undesirable effects such as the removal of the contact surfaces of the shelves (leading to uneven contacts), increased wear of the contact surfaces of shelves and loss of load reduction effects, etc. In addition, at the end of the section of the blade profile, tensile stress increases at points A and B which adversely affect design safety. However, they can be reduced by applying the rounding sizes in the connection between the shroud shelf and the blade profile (Fig. 7). It is therefore desirable to leave the gravity centre unchanged in the circumferential direction or to select it in a small range. Here is the possibility of carrying out separate studies with the angles of the shelving contacts setting, choosing

their optimal values. Considering the above mentioned, as well as the changing operating conditions of the aircraft engines and the changing conditions of the flight, the determination of the optimal gravity centre of the shroud shelf becomes a rather complex task involving a multiplex solution using modern computer modelling methods.

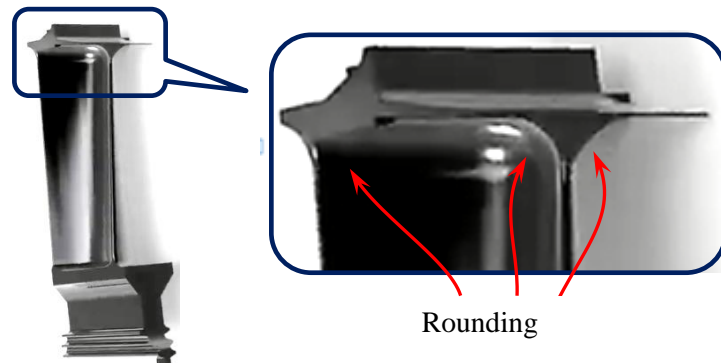


Fig. 7. Inner corner rounding between the blade profile section and the shroud shelf.

#### IV. RESULTS

The study describes an unloading of the base part of the turbine blade from bending stresses and an additional load reduction from residual bending stresses in the middle of the blade on the “back” side. The realised sample calculations with the different variations of the gravity centre placement of the shroud shelf allow to conclude that the results obtained generally demonstrate the possibility of load reduction from residual bending stresses in the middle of the blade. In addition, the stress jumps at the end of the blade (see Fig. 6, points b, d, e, f) will decrease significantly due to rounding in the inner corner between the shroud shelf and the blade profile (see Fig. 7). For the simplification of the given calculations, rounding was not taken into account. Fig. 6 b, d, e, f. shows stress jumps. The results obtained can be taken as a basis for further studies in this direction, using precise modern computer programs, as well as developing experimental equipment for further laboratory research. The blade unload technique from residual bending stresses is more suitable for surface gas turbine engines, because they have constant atmospheric conditions that facilitate the calculation procedure. Such engines have larger dimensions, followed by the turbines with longer blades that increase the load effect of residual bending stresses.

#### REFERENCES

- [1] I. Ozoliņš, Ē. Ozoliņš and V. Fedotova, “Development of a Method for Calculating the Working Blade Stress Profile of the Aviation Gas Turbine Engine for Student Training”. *Transport and Aerospace Engineering Journal*. vol. 6, no. 1, pp. 55–66, 2018. <https://doi.org/10.2478/tae-2018-0007>
- [2] A. A. Inozemcev and V. L. Sandrackij, *Gazoturbinnye dvigateli*. OAO Aviadvigatel. Perm, 2006.
- [3] R. J. Boyle, L. M. Agricola, A. H. Parikh, A. A. Ameri and V. K. Nagpal. “Shrouded CMC Rotor Blades for High Pressure Turbine Applications”. *ASME Turbo Expo 2018: Turbomachinery Technical Conference and Exposition*. No. GT2018-76827, pp. V02BT41A028; 10 pages. <https://doi.org/10.1115/GT2018-76827>
- [4] Y. Assoul, S. Benbelaid, V. Šijački-Žeravčić, G. Bakić and M. Đukić, “Life Estimation of First Stage High Pressure Gas Turbine Blades”. *Scientific Technical Review*, vol. LVIII, no. 2, pp. 8–13, 2008.
- [5] R. I. Stephens, A. Fatemi, R. R. Stephens and H. O. Fuchs, *Metal Fatigue in Engineering*. New York, 2001.
- [6] Z. Liu, Z. Chen and J. Chen, “The Strength Analysis of CFM56 Engine Blade”. *MATEC Web of Conferences (ICMAA)*, vol. 166, 2018. <https://doi.org/10.1051/mateconf/201816604001>
- [7] V. A. Frolov, V. G. Kocenko and S. B. Luzkov, *Raschet lopatok kompressora i turbiny na staticheskuju prochnost i kolebanija*. Samara: SGAU, 2000.
- [8] M. L. Kuzmenko, V. S. Chigrin and S. E. Belova, *Staticseskaja prochnost rabochih lopatok i diskov kompressorov i turbin GTD*. Uchebnoe posobie. Rybinsk: RGATA, 2005.
- [9] G. S. Skubacevskij, *Aviacionnye gazo-turbinnye dvigateli. Konstrukcija i rascet detalej*. Moscow: Mashinostroenie, 1981.

- [10] B. E. Vasiljev and L. A. Magerramova. "Analiz vlijanija konfiguracii bondaznih polok lopatok turbin perspektivnih dvigatelei na procnostnije karakteristiki". *Vestnik YGATY*, 2015.
- [11] D. Z. Yu, D. H. Wen and H. R. Zhang, "Structural static analysis of gas turbine blade and disk of an aeroengine". *Structure & Environment Engineering*, 2012.
- [12] R. Fernandes, S. El-Borgi, K. Ahmed, M. I. Friswell and N. Jamia, "Static fracture and modal analysis simulation of a gas turbine compressor blade and bladed disk system". *Advanced Modeling and Simulation in Engineering Sciences*, vol. 3, no. 1, December 2016. <https://doi.org/10.1186/s40323-016-0083-7>
- [13] D. V. Hronina (ed.), *Konstrukcia i proektirovanie aviacionnyh gazoturbinnih dvigatelej*. Moscow: Mashinostroenie, 1989.
- [14] A. S. Vinogradov and G. Kartashov, *Konstruirovanie lopatok i diskov AD i EU*. Samara: RIO SGAU, 2007.
- [15] N. I. Starcev, *Konstrukcia i proektirovanie turbokompressora GTD*. Uchebnoe posobie. Samara: RIO SGAU, 2006.
- [16] V. F. Haritonov. *Materialy detalej aviacionnyh gazoturbinnih dvigatelej*. UFA: UGATU, 2004.



**Ēriks Ozoliņš**, Dr. sc. ing.

Education: 2000–2003: Riga Technical University, Aviation Institute, PhD in Engineering; 1998–2000: Riga Technical University, Aviation Institute, M. sc.; 1994–1998: Riga Aviation University, B. sc. in Engineering.

Work experience: 2003–2005: Riga Technical University Aviation institute assistant; 2005–2008: Riga Technical University Aviation institute lector; 2008–present: Riga Technical University Aviation institute doctor.

Research interests: acoustic emission, material strength, structural health monitoring.

Publications: about 30 scientific and educational papers. Participation in one European projects (AISHA).

Address: Institute of Aeronautics, Faculty of Mechanical Engineering, Transport and Aeronautics, Riga Technical University, Lauvas 8, Riga, LV-1019, Latvia.

Phone: (+371) 67089990

E-mail: Eriks.Ozolins@rtu.lv



**Ilmārs Ozoliņš**, Dr. sc. ing.

Education: 2000–2004: Riga Technical University, Aviation Institute, PhD in Engineering; 1998–2000: Riga Technical University, Aviation Institute, M. sc.; 1994–1998: Riga Aviation University, B. sc. in Engineering.

Work experience: 2005–2008: Riga Technical University Aviation institute assistant; 2008–2010: Riga Technical University Aviation institute lector; 2010–present: Riga Technical University Aviation institute doctor.

Research interests: Aviation gas turbine and piston engines, Propellers, Composite materials.

Publications: about 30 scientific and educational papers. Participation in one European projects (AISHA).

Address: Institute of Aeronautics, Faculty of Mechanical Engineering, Transport and Aeronautics, Riga Technical University, Lauvas 8, Riga, LV-1019, Latvia.

Phone: (+371) 67089990

E-mail: Ilmars.Ozolins@rtu.lv



**Līga Ramāna** graduated from the Faculty of Physics and Mathematics, University of Latvia, in 1994. At 1996 obtained Mg. Math. at University of Latvia. She received the Dr. Math. degree from University of Latvia in 2004.

She has a work experience as a Laboratory Assistant at Riga Technical University, Assistant Lecturer, Lecturer, Docent and Associated Professor at Latvian University of Agriculture (1996–2013), Lecturer and Docent at University of Latvia (1999 – 2008), researcher at University of Latvia (2010–2012). Since 2013 she is an Associated Professor at Riga Technical University, Institute of Applied Mathematics, Faculty of Computer Science and Information Technology.

Research interests: Modern Elementary Mathematics, Mathematics Didactic, Mathematics and it's Applications for Engineering students.

Address: Institute of Aeronautics, Faculty of Mechanical Engineering, Transport and Aeronautics, Riga Technical University, Lauvas 8, Riga, LV-1019. Latvia.

Phone: (+371) 67089990

E-mail: liga.ramana@rtu.lv